X- AND γ-RAY MEASUREMENTS DURING THE 1972, AUGUST 2 AND 7 LARGE SOLAR FLARES

R. TALON and G. VEDRENNE

Centre d'Etude Spatiale des Rayonnements – B.P. 4057–31029, Toulouse Cedex, France

and

A. S. MELIORANSKY, N. F. PISSARENKO, V. M. SHAMOLIN, and O. B. LIKIN

Institut de Physique Spatiale I.K.I., Académie des Sciences d'U.R.S.S., Moscou, U.R.S.S.

Abstract. The solar X- and gamma-ray experiment aboard Prognoz 2 recorded solar gamma-radiation bursts during the 1972, August 2, 4 and 7 events. This work analyses the general evolution of the August 2 and 7 events and the possible evidence for γ-ray lines during these two events.

I. The Experiment

The satellite Prognoz 2 was launched on 29 June 1972 for the purpose of studying the effects of solar activity. The satellite orbit is inclined at 65°, with an apogee of 200 000 km and a perigee of 1000 km.

At launch time the projection of the abside line on the ecliptic plane was close to the direction of the Sun.

The scientific equipment aboard the satellite consists of detectors for studying temporal changes in electromagnetic radiation and charged solar particles.

For the large events of 1972, August 2 and 7, data were analyzed from the RS 1 and SGL 1 X-ray spectrometers, a gamma radiation spectrometer from the Signe 1 experiment, and several charged particle detectors, all of which are described below.

The RS 1 spectrometer consists of a proportional counter shielded by passive (copper) and active (gas counter) anticoincidences. Its volume is 400 cm^3, and it is filled with a mixture of 90% xenon and 10% methane under a pressure of approximately 0.8 atm. The 0.5 cm^2 area window of the counter is made of Beryllium 60 μ thick.

The count rates of this detector were recorded in four energy ranges:

$$\Delta E_1 \simeq 4.1\text{–}9.7 \text{ keV}, \qquad \Delta E_2 \simeq 9.7\text{–}19.0 \text{ keV}$$
$$\Delta E_3 \simeq 19.0\text{–}33 \text{ keV}, \qquad \Delta E_4 \simeq 33\text{–}54 \text{ keV} \tag{1}$$

The detailed characteristics of the apparatus have been given elsewhere (Grigorov *et al.*, 1974).

The SGL 1 spectrometer is designed to measure the spectrum of X-rays in the range 38–340 keV. This energy interval is divided as follows:

$$\Delta E_5 \simeq 38\text{–}77 \text{ keV}, \qquad \Delta E_6 \simeq 77\text{–}130 \text{ keV}$$
$$\Delta E_7 \simeq 130\text{–}250 \text{ keV}, \qquad \Delta E_8 \simeq 250\text{–}340 \text{ keV} \tag{2}$$

This detector is a scintillation counter composed of a Cs I (Tl) crystal, 39 mm in diameter and 8 mm thick, and an FEO 53 photomultiplier. The detector is shielded

over 4π by a plastic scintillator 0.5 cm thick. The entry window consists of a sheet of 0.1 mm aluminum and 0.1 mm of reflective material. In addition to the X-ray data, this detector gives information on events when γ-rays (energy > 340 keV) and charged particles interact in the main detector. The detailed description of this SGL 1 apparatus is given elsewhere (Kudriatsev *et al.*, 1973).

In the Signe 1 apparatus designed to study solar gamma radiation and neutrons, a Stilbene scintillator, 38.1 mm in diameter and 38.1 mm high, shielded by a plastic scintillator, is used. The Compton electrons and recoil protons due respectively to photon and neutron interactions in the stilbene are detected by a Radiotechnique 416 F photomultiplier. The anticoincidence plastic scintillator coupled to a RCA 4441 A photomultiplier rejects charged particles. Pulse shape discrimination separates electrons from protons. The gamma radiation is measured in the following intervals:

$$
\begin{aligned}
&E_9 \simeq 0.4\text{--}0.7 \text{ MeV}, &&E_{10} \simeq 0.7\text{--}1 \quad \text{MeV} \\
&E_{11} \simeq 1 \;\;\text{--}1.6 \text{ MeV}, &&E_{12} \simeq 1.6\text{--}2.4 \text{ MeV} \\
&E_{13} \simeq 2.4\text{--}2.9 \text{ MeV}, &&E_{14} \simeq 2.9\text{--}3.9 \text{ MeV} \\
&E_{15} \simeq 3.9\text{--}8.1 \text{ MeV}, &&E_{16} \simeq 8.1\text{--}11.8 \text{ MeV}
\end{aligned} \tag{3}
$$

The detector works in two successive modes:
(1) Recording gamma photons between $\Delta E_9\text{--}\Delta E_{14}$
(2) Recording gamma photons between $\Delta E_{14}\text{--}\Delta E_{16}$
Each phase lasts 82 min; a more detailed description of this experiment has appeared in Vedrenne *et al.* (1973).

The count rate is recorded in the RS 1 and SGL 1 apparatus and in mode (1) of the Signe 1 apparatus once every 41 s and in mode (2) of the Signe 1 apparatus once every 160 s.

Data for proton fluxes were obtained above 500 MeV from a Cerenkov counter (Blioudov *et al.*, 1974) and above 15 MeV from an STS 5 discharge counter. The general characteristics of these detectors are given in Table I.

TABLE I

Detector characteristics

Detector	Energy range	Area (cm²)	Opening angle
(1) Be 60 μ window proportional counter	2.3–28 keV	0.5	20°
(2) CsI(Tl) crystal scintillation counter, 8 mm thick, 39 mm diameter	38–340 keV	10	45°
(3) Stilbene scintillation counter 38.1 mm diameter, 38.1 mm thick	0.35–11.8 MeV	17.1	4π
(4) STS 5 gas discharge counter	Protons $E > 15$ MeV Electrons energy > 1 MeV	2.15	2π
(5) Cerenkov counter	Protons $E \geqslant 500$ MeV Protons $E \geqslant 100$ MeV	5 8	40° 30°

II. Experimental Results

A remarkable series of complex flares appeared in early August 1972, in particular on August 2, 4 and 7.

We observed these events in X-rays, but the time resolution (41 s) did not permit a fine time analysis. However the use of a satellite with a very eccentric orbit pointed at the Sun allowed us to follow the large scale evolution of the X- and gamma-radiation for all the events. Since the observations took place when the satellite was out of the magnetosphere, an increase in the background count rate was observed on all the detectors when the solar charged particles arrived near the Earth. One exception was the August 2 events, which will be analyzed first. In this case no contamination from these particles was observed.

(a) AUGUST 2 EVENTS

(i) *Description of The Events*

(α) *First event*. This event begins at 3 10 and shows a maximum at 3 30. This large, early event is associated with a type 1B burst from the Mac Math region 11976 located at 13°N and 35°–37°E.

The SGL 1 X-ray spectrometer recorded the beginning of the event at 3 11 20, with the first maximum (~ 1 photon cm^{-2} s^{-1} keV^{-1}) at 3 30 in the energy range 38–77 keV. For this energy range a less pronounced secondary maximum (~ 0.5 photons cm^{-2} s^{-1} keV^{-1}) appeared at 4 03 51.

The decreasing time of this event is about 55 min and the total duration is 143. (Figure 1).

The radio measurements we used were made at the Manila Observatory between 606 and 8800 MHz (Castelli *et al.*, 1973). High frequencies time profiles particularly at 8800, 4995 and 2695 MHz, coincide well with the X-ray measurements. The second radio maximum (~ 400) can be seen to be higher than the first at 4995 and 2695 MHz.

This radio burst has the usual characteristics of a proton flare burst (Castelli *et al.*, 1973):

– slow rise to maximum, long duration;
– values greater than 1000 fu at $\lambda = 3$ cm;
– intense meter wavelength emission;
– typical U-shape of the frequency spectrum at the time of the 2 maxima (Figure 2).

In spite of these characteristics, the Signe 1 experiment did not measure any gamma emission in the energy range 0.35–3.9 MeV.

An X-ray spectrum corrected for detector effects can be obtained from the experimental data using a Monte-Carlo program (Bui-Van *et al.*, 1973). This spectrum has the form $AE^{-\alpha}$ with $A = 6.3 \times 10^{8}$ photons cm^{-2} s^{-1} keV^{-1} and $\alpha = 4.5$.

Knowing this spectrum one can deduce the energy associated with the electron component using the method by Brown (1972). For electrons with energy $E_e > 10$ keV, an energy of $\sim 10^{30}$ ergs is obtained in the impulsive injection model and 5×10^{29} ergs s^{-1}
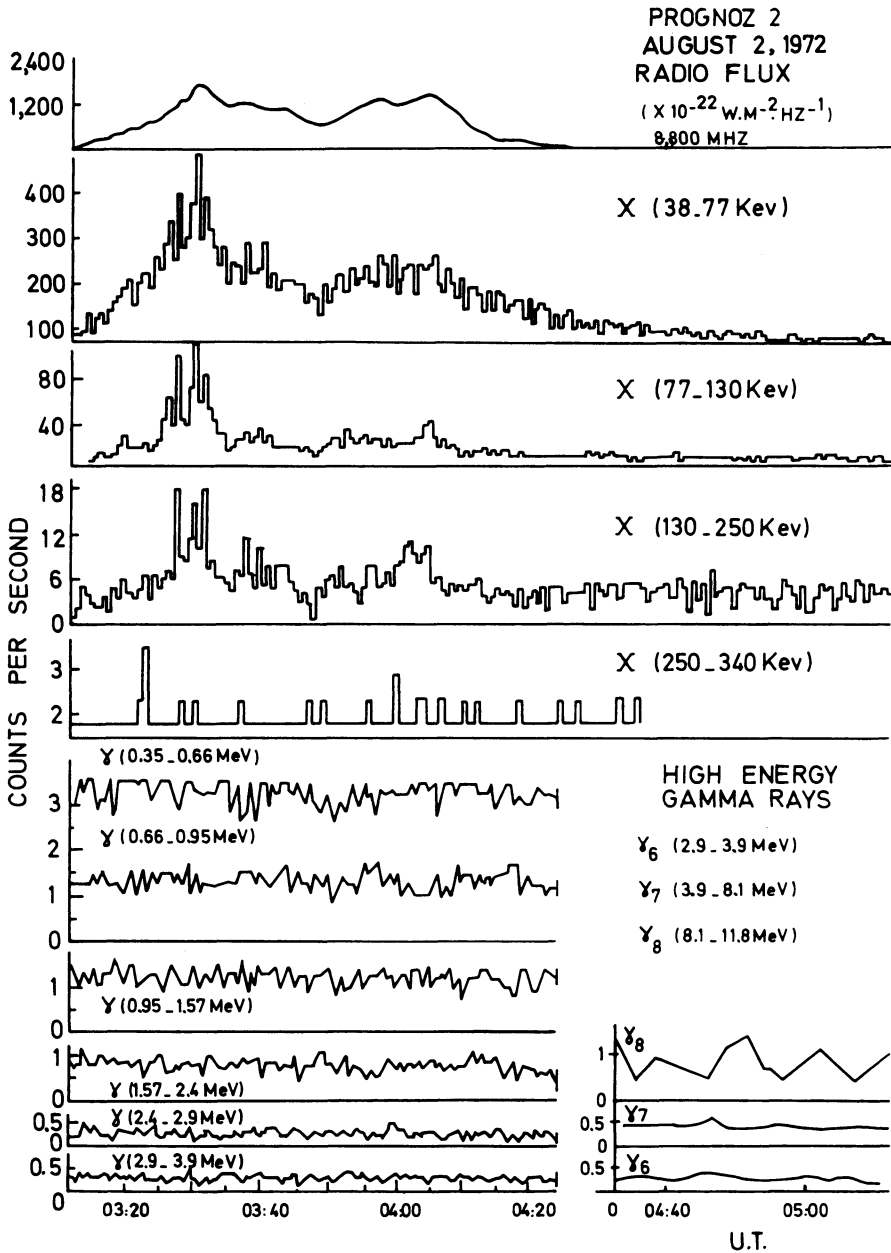
Fig. 1.   Time profile of the X- and γ-ray measurements of the SGL 1 and Signe I experiments at
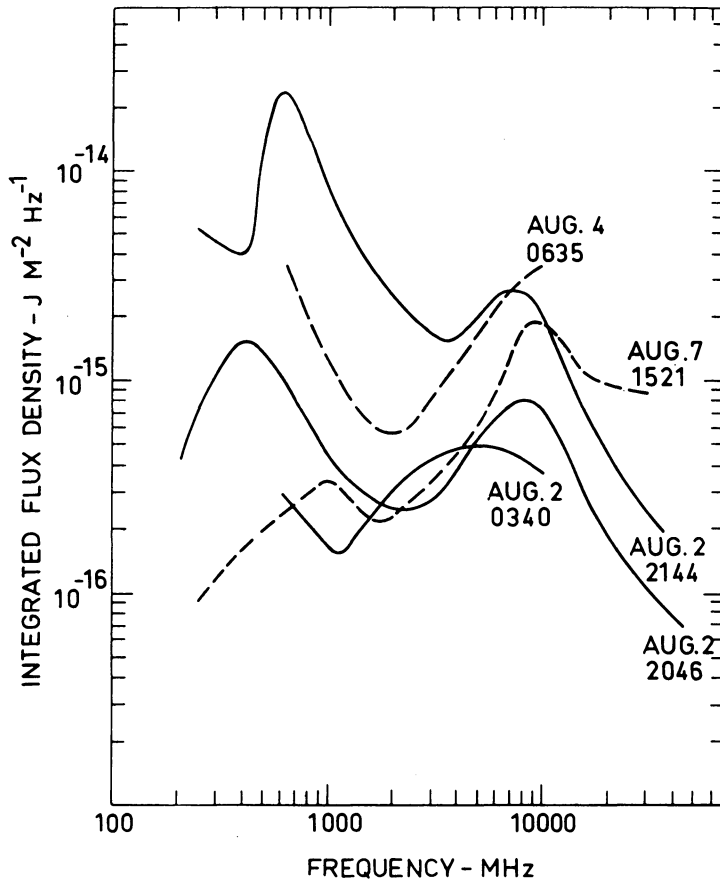0300 UT in 1972, August 2.

Fig. 2. Integrated flux density for proton associated bursts of August 1972. Curves derived from Sagamore Hill and Manila Data.

in the continuous injection model. These values, as has already been observed several times, are well above the energy calculated from the radio fluxes (4.7×10^{24} erg in the range 600–8800 MHz).

(β) *Second event.* This very brilliant, impulsive Type 1B flare was located at 15°N and 25–26°E.

This event, observed in X-rays by our experiment and also by OSO 7 and TD 1 (Datlowe and Peterson, 1973; Van Beek *et al.*, 1973), was short. In the 33–77 keV band the X-ray emission appears at 18 38 18 and lasts about 8 min, the maximum, at 18 40, is 0.77 photons cm^2 s^{-1} keV^{-1}. At higher energies, the X-ray emission is much shorter, about 41 s (Figure 3).

During the event the microwave spectrum was steeply rising to high frequencies which may indicate a low source height. At 18 40, about one minute after the maxi-
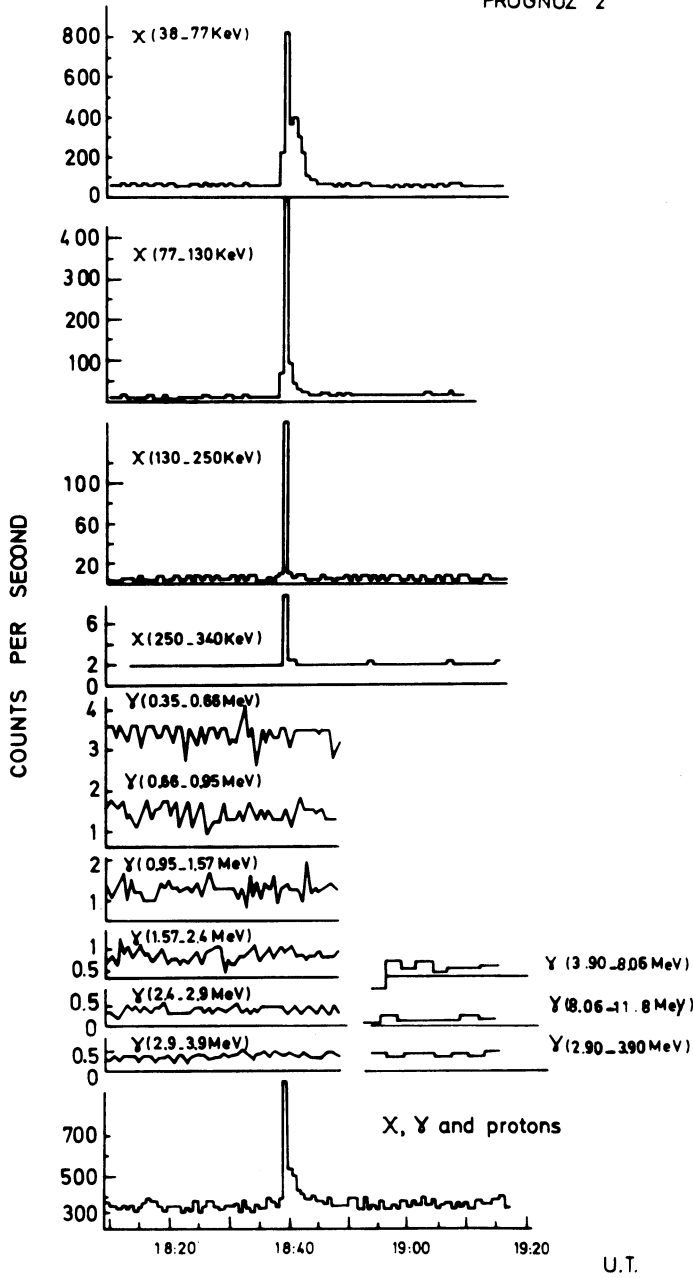
R. TALON ET AL.

Fig. 3.   The event of 1972, August 2, 1840 UT.

mum, a rapid decrease of the flux around 35 GHz was observed. This decrease coincided with the end of the 3825 Å flash (Zirin and Tanaka, 1973).

Comparisons at optical (3835 Å), X- and radio frequencies are given by Zirin and Tanaka (1973) and their conclusion is that the thick target X-ray emission model is more consistent than the thin target model for this impulsive flare.

Using our Monte Carlo program, we have found the incident photon spectrum. At the time of maximum it has the form $AE^{-\alpha}$ with $\alpha = 3.7$ and $A = 1 \times 10^7$ photons cm^{-2} s^{-1} keV^{-1}. These values are in good agreement with those of OSO 7 (Datlowe and Peterson, 1973). The energy dissipated by the electrons in collisions has been computed using Brown's method (Brown, 1972). For the thick target model which applies best to this event, as Zirin and Tanaka (1973) have noted the energy involved at the time of the maximum is about 3×10^{29} erg s^{-1} for electrons above 10 keV.

During this event no gamma emission was observed.

(γ) *Third event*. This event is associated with a type 1B flare from the MacMath region 11976, 13° N, 26–28° E and is the most structured of all the August 2 X-ray events. It is, however, similar to the 03 10 flare is some ways: it is a long-lived, slowly rising flare. The characteristics of this flare are already given by Zirin and Tanaka (1973): reached maximum at about 2005 and gave a modest hard X-ray burst; at 2020 there was a new increase in area and brightness. The hard X-ray flux increased, and at 8800 MHz a large flux (6600 fu) was observed. The Hα front spread steadily to a maximum at 20 50 UT. At 21 40 the highest radio and X-ray flux peak can be noticed.

The entire event was observed by our X-ray detectors (Figure 4). For the first part of the event, OSO 7 could not give results because the satellite was in the Earth's shadow between about 20 30 and 21 10. However, during the period from 21 10 to 22 00 the second part of the event was observed by this satellite and a large continuum was reported up to 600 keV. Unfortunately at the time of this second large maximum in X-rays, our gamma ray detector was in a calibration mode during which the anti-coincidence was not working. Nevertheless it seems that an increase in the ΔE_9 and ΔE_{10} channels appeared at about 21 40. But since these are the only data before the change in operating mode, no conclusive result is possible for this part of this event.

So we will concentrate on the first part of the event at 20 40. Several bursts, particularly in the ranges 38–77 keV and 77–130 keV can be noted (Figure 5). This type of phenomenon can also be found in the August 7 events. The maximum for this event takes place at 20 46 36 in the 38–77 keV channel. At the time of the maximum the X-ray spectrum has the following form: $8.10^6 \, E^{-3.3 \pm 0.3}$ photons cm^{-2} s^{-1} keV^{-1}. The calculations, again using the method developed by Brown (1972), give values for the electron energy of 2×10^{27} erg s^{-1} for $E_e > 40$ keV and 10^{33} electrons s^{-1} for $E_e > 100$ keV.

It is interesting to note that during this first part of the event, at about 20 45 a very high increase in the gamma-ray flux above 350 keV (Figures 4 and 5) was observed. Figure 5 also shows the variation in radio flux at 8800 MHz. The good agreement
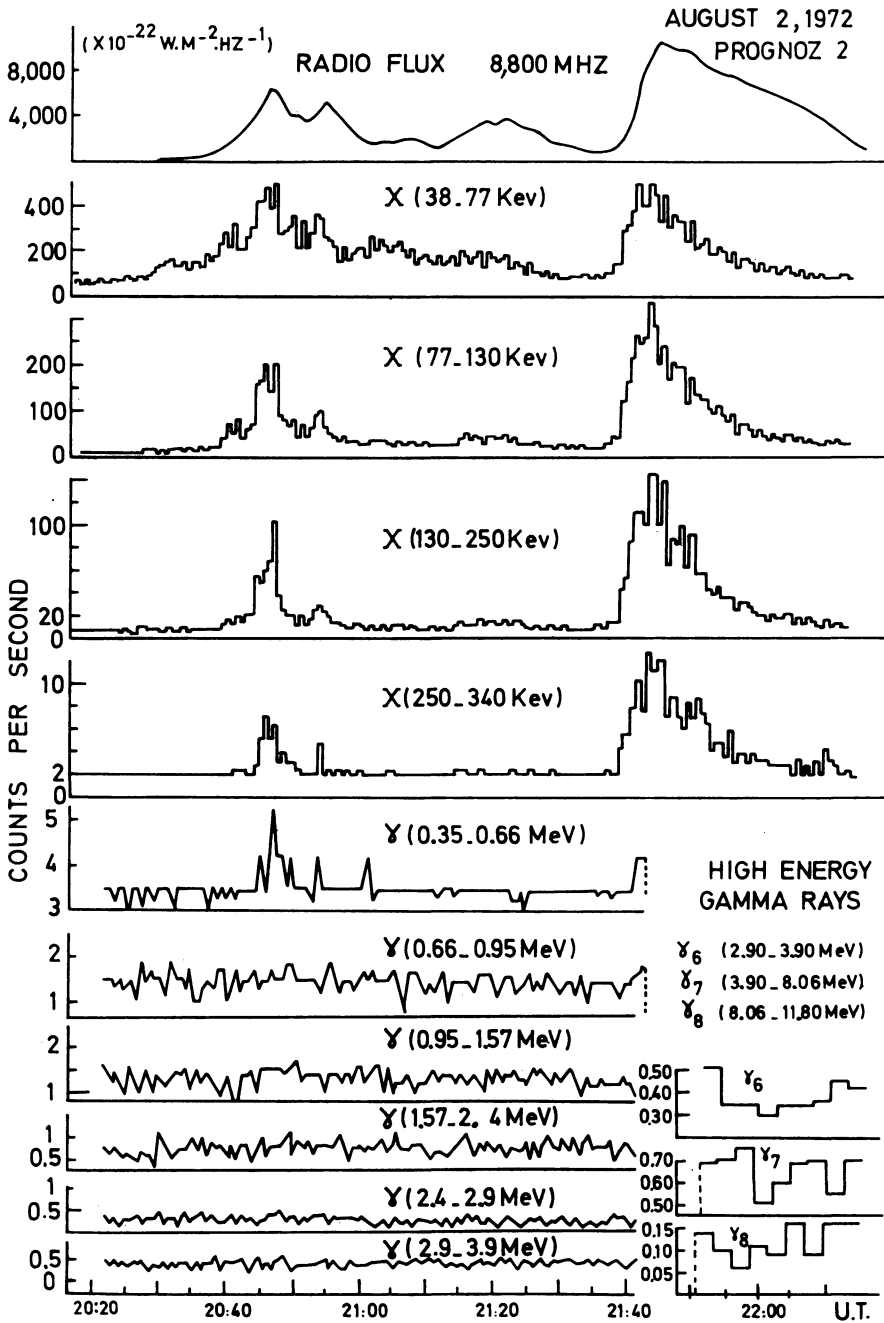
Fig. 4.   Time profiles of the August 2, events 20 40 and 21 40 UT.

between the time variations of the count rate observed in the ΔE_9 channel and those of the radio and X-ray fluxes beyond 70 keV is evident. In addition, the radio spectrum can be seen to show the same characteristics as that of the 3 30 event (Figure 2). The U-shape of this spectrum is often taken to indicate the presence of charged particles.
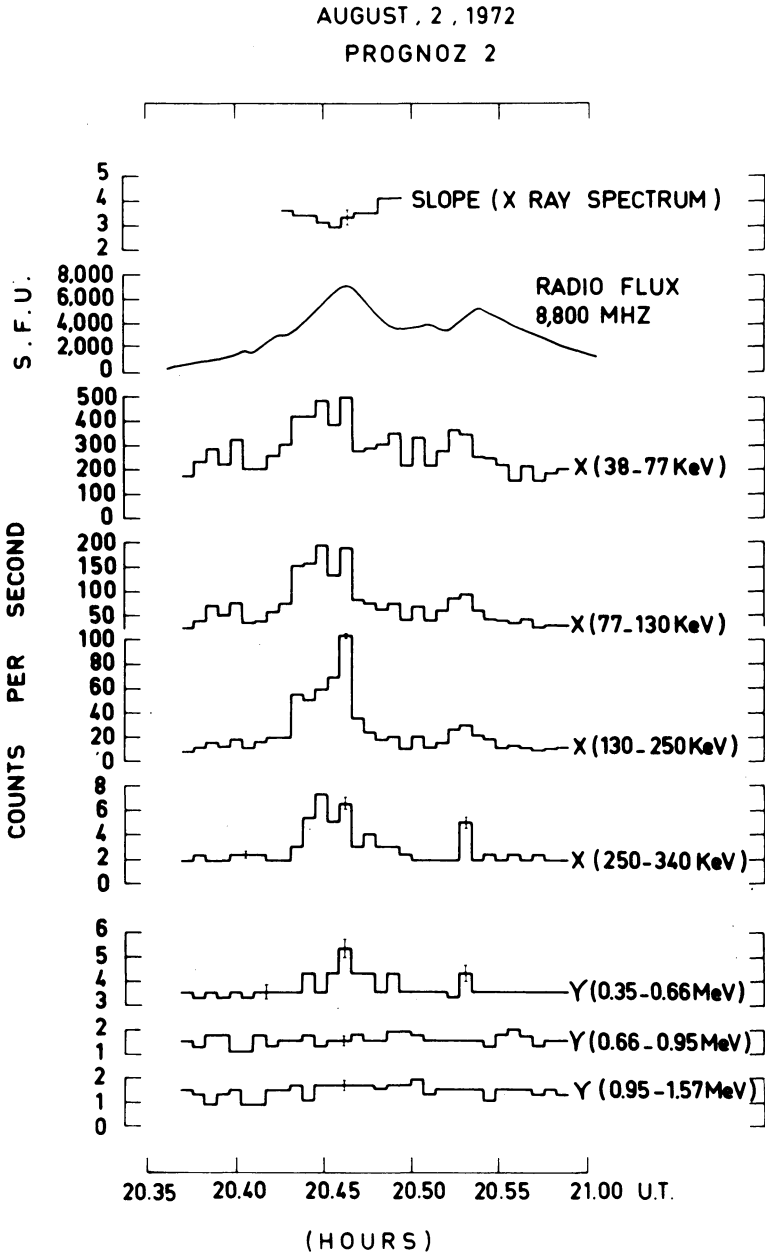

Fig. 5.   A detailed time profile of the 2040 August 2 event.

In order to interpret the flux increase in the ΔE_9 channel and to determine whether this flux increase could be due in part to the presence of a line a 0.511 MeV, it is necessary to calculate the contribution of the continuum in the ΔE_9 channel. We assume that the spectrum is a power law and that it can be extrapolated to higher energy.

(ii) POSSIBILITY OF A CONTRIBUTION OF THE 511 keV LINE

The X-ray spectrum calculated has the form $8 \times 10^6 \, E^{-3.3 \pm 0.3}$ photons cm^{-2} s^{-1} keV^{-1}. The error in the exponent is calculated assuming a possible deviation of 3σ in the experimental values obtained by the SGL 1 detector. Using this spectrum, we estimate the increase we would have had in the ΔE_9 channel if the event had included only continuum. This increase is only detectable in the first channel (ΔE_9), but it is not enough to explain the increase observed. Table II gives the 41 s count rate values obtained in the ΔE_9 and ΔE_{10} channels at the time of the maximum:

TABLE II

Counts observed during 41 s at the time of maximum intensity

Energy channel	Observed counts	Background	Continuum contribution (of solar origin)	Possible 0.5 MeV line contribution
ΔE_9	237	155	24	58
ΔE_{10}	56	56	5	—

While this table shows a significant contribution which could be attributed to the 511 keV line, it is necessary to take into account the errors in determining the continuum spectrum: specifically the continuum contribution in ΔE_9 is 24 ± 13 cts (41 s)$^{-1}$.

For a total detection efficiency of 33% the efficiency in the channel ΔE_9 is 14%, so the excess observed in this channel leads to a flux associated with the 511 keV line which is:

$$\phi_{0.511} = 0.6 \pm 0.5 \text{ photons cm}^{-2} \text{ s}^{-1}. \tag{4}$$

Using the calculations of Ramaty and Lingenfelter (1973) which give a relation between the 511 keV and 2.23 MeV fluxes (Figures 6, 7) we can estimate the 2.23 MeV line contribution in our detector if we know its sensitivity to this line.

The Table III gives the efficiencies of various energy channels for detecting 2.23 MeV gamma photons.

TABLE III

Efficiencies of the various channels
for 2.23 MeV photons

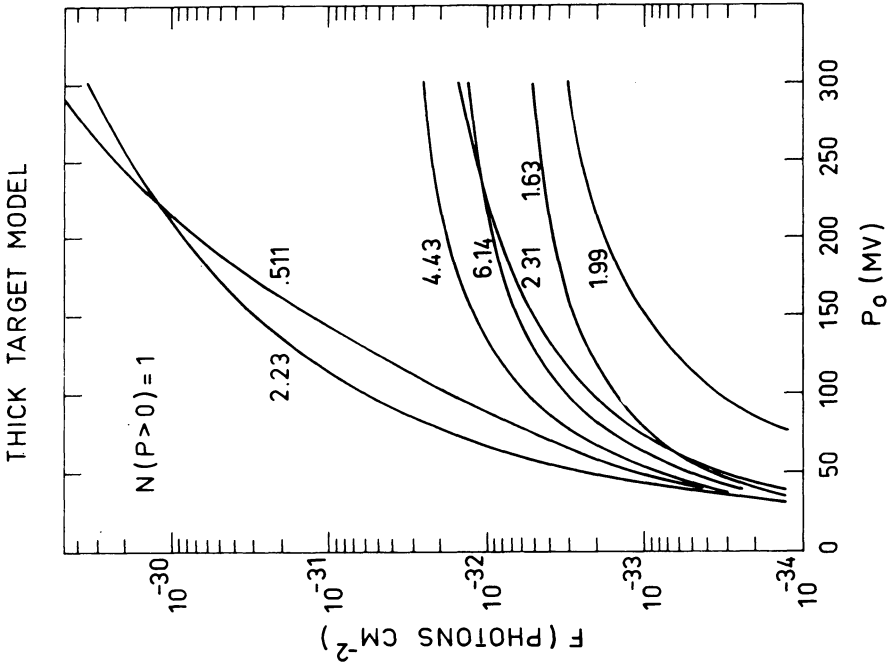| Energy channel	ΔE (keV)	Efficiency %
ΔE_9	0.4–0.7	1.6
ΔE_{10}	0.7–1	1.7
ΔE_{11}	1–1.6	3.4
ΔE_{12}	1.6–2.4	7.1
ΔE_{13}	2.4–2.9	0.6

Fig. 7. γ-ray line flux normalized to one incident proton for the thick-target model.
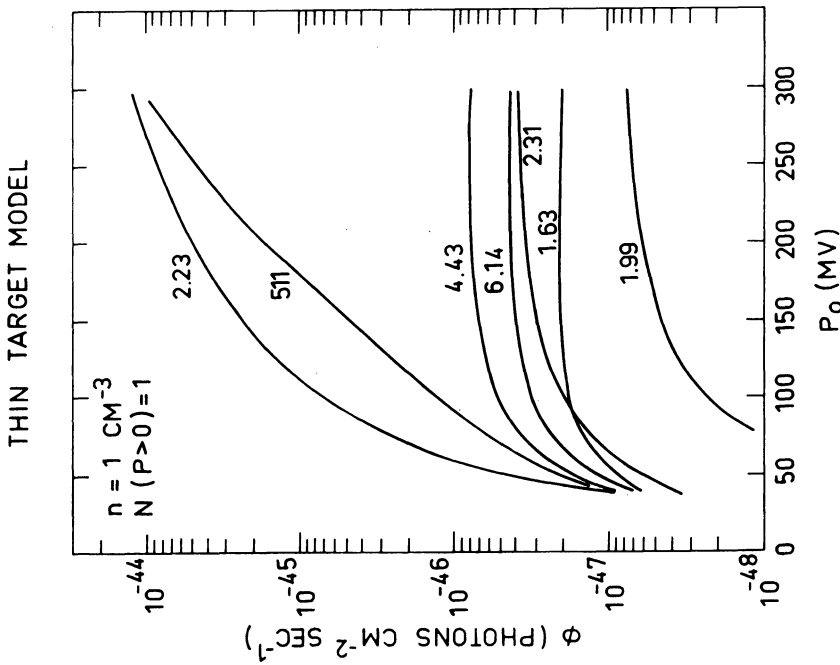

Fig. 6. γ-ray line flux normalized to 1 cm^{-3} and for 1 incident proton for the thin-target model.

The sensitivity of our detector in the ΔE_{12} channel where the efficiency is greatest, is 0.15 photons cm^{-2} s^{-1} at 2.23 MeV at the 1 σ level and 0.33 photons cm^{-2} s^{-1} at the 2 σ level for 41 s.

The calculation of Wang and Ramaty (1974) enables us to specify the expected fluxes at 2.23 MeV for different rigidities in both thick and thin target models, knowing the 511 keV flux. The values are given in Table IV.

TABLE IV
Expected photons cm^{-2} s^{-1} at 2.23 MeV

Proton rigidity	Thick target model			Thin target model		
	ϕ 0.511 MeV (photons cm^{-2} s^{-1} keV^{-1})					
	0.1	0.6	1.1	0.1	0.6	1.1
40 MV	0.08	0.4	0.8	0.05	0.3	0.5
50 MV	0.1	0.6	1.2	0.1	0.6	1.1
100 MV	0.18	1	1.9	0.3	1.6	2.8

Under these conditions, the absence of a 2.23 MeV line contribution in the ΔE_{12} channel (where efficiency at 2.23 MeV is highest) makes it possible to define an upper limit for the gamma flux value at 0.5 MeV, assuming that Wang and Ramaty's model does indeed represent the gamma line emission processes.

The upper limits to the photon flux at 0.5 MeV are then:

Proton rigidity	Thick-target	Thin-target	
40 MV	0.44 photons cm^{-2} s^{-1}	0.66 photons cm^{-2} s^{-1}	(5)
50 MV	0.28 photons cm^{-2} s^{-1}	0.33 photons cm^{-2} s^{-1}	
100 MV	0.18 photons cm^{-2} s^{-1}	0.12 photons cm^{-2} s^{-1}	

We estimate next the characteristic rigidity of this event in order to give a more accurate upper limit.

(α) *Determination of the event's characteristic rigidity.* The rigidity can be estimated using measurements from Explorer 41 (Bostrom *et al.*, 1972) but for the August 2 event there is a problem: the flare responsible for the proton emission is located to the east on the Sun. Since the lateral diffusion of these protons is low compared to the diffusion along the magnetic field line, it is impossible to attribute the proton flux increase to any particular August 2 event; as we have seen, all these events can be responsible for proton emission. The Explorer 41 data however, indicate a plateau at 1200 UT August 3. This configuration being typical of the events occurring to the east on

the Sun. We have therefore determined the characteristic rigidity using the Explorer 41 data, assuming that this rigidity was conserved in the scattering.

The flux values measured under these conditions will necessarily be lower than those at the Sun. The observed fluxes were as follows:

Proton energy E	Integral proton flux at the Earth $J(>E)$	
>10 MeV	500 protons cm^{-2} s^{-1}	(6)
>30 MeV	37 protons cm^{-2} s^{-1}	
>60 MeV	12.5 protons cm^{-2} s^{-1}	

From these values one can deduce the proton density in the interplanetary medium $U(P)$, since, if this density is put into the form $U(P) \simeq \exp(-P/P_0)$ then

$$U(>P) = J(>P) \cdot \frac{mc}{e} \cdot (P + P_0)^{-1} \text{ with } \frac{mc}{e} = 3.12 \times 10^{-8}. \qquad (7)$$

Under these conditions and with the above mentioned reservations the characteristic rigidity can be estimated at between 40 and 50 MV.

(β) *Number of protons emitted in the event assuming a gamma-ray line emission.* The estimate of the number of protons at the Sun in the thick target model are obtained for an average rigidity of 45 MV and for 511 keV fluxes of 0.1 photons cm^{-2} s^{-1} and 0.35 photons cm^{-2} s^{-1}. In this case as the event lasts 41 s, the total number of protons according to Figure 7 lies between 5×10^{33} and 2×10^{34} protons.

These values can be compared to that deduced from observations made at the Earth. But we have pointed out that the main problem lies in the low value of proton fluxes measured at the earth when emitted east of the Sun. However it is possible to give an approximation of these fluxes (>10 MeV) by using the curve of Straka (1970) (Figure 8). In order to do this, we have determined the energy from radio observations at 8800 MHz (8×10^{-16} J. m^{-2} Hz^{-1}); according to this curve, a proton flux of about 600 p cm^{-2} s^{-1} sr^{-1} results, or 15 times the value of the fluxes measured. Using this proton flux and a volume occupied by the particles in interplanetary space of 10^{39} cm^3 (Ramaty and Lingenfelter, 1973), the number of protons is equal to 2.6×10^{34}.

(γ) *Ambient density of the solar atmosphere.* In the thin target model taking the 0.511 MeV line flux between 0.1 and 0.45 photons cm^{-2} s^{-1} one obtains for nN (Figure 6):

$$7 \times 10^{45} < nN < 3 \times 10^{46}. \qquad (8)$$

Thus, taking the value derived from measurements at the Earth for the number of protons, the number density of the ambient solar material (cm^{-3}) becomes:

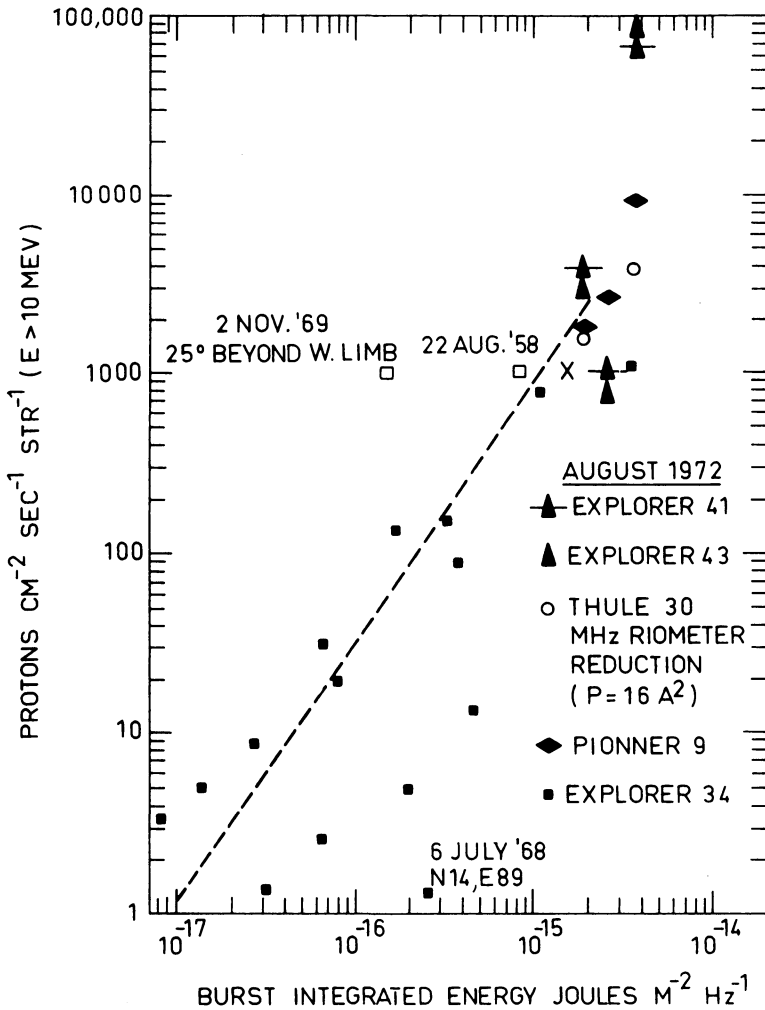$$3 \times 10^{11} < n < 1 \times 10^{12}. \qquad (9)$$

Fig. 8.   Burst integrated energy at 8800 MHz vs proton flux.

(δ) *Energy involved during the flare.* First we consider the thick-target model. Assuming that the proton population has a spectrum with the form $N(P) = P_0^{-1} \exp(-P/P_0)$, the average proton energy is P_0^2/Mc^2 or 3.4×10^{-6} erg. The total energy involved is then:

$$1.7 \times 10^{28} \text{ ergs} < W_T < 6.8 \times 10^{28} \text{ ergs} \tag{10}$$

In order to find the energy involved in the thin target model, we compute the energy W dissipated per unit time by a proton, in a medium having a density of 1 cm^{-3} (Ramaty and Lingenfelter, 1973).

The results are presented in Table V. Using the value 1.9×10^{-18} erg s^{-1} for a rigidity of 45 MV and the values of nN previously calculated, we obtain the energy

TABLE V

Energy dissipated by protons in the
thin-target model

Rigidity P_0 (MV)	Energy dissipated $W \times 10^{-18}$ erg s^{-1}
20	2
30	2
40	1.9
60	1.8
80	1.6
100	1.5
120	1.4
200	1.2
300	1.1

involved, E, for an event lasting 41 s:

$$5 \times 10^{29} \text{ ergs} < E < 2 \times 10^{30} \text{ ergs} . \tag{11}$$

(b) AUGUST 7 EVENT

(i) *Description of The Event*

In the MacMath region 11976 with which the events of August 2 and 4 have already been associated, an event appeared on August 7. Figure 9 shows recording from RS 1, SGL 1, and Signe 1 detectors as well as the proton detector data for the burst period. For purpose of comparison, the same figure shows radio fluxes at a frequency of 15 400 MHz (Castelli *et al.*, 1973), as well as the periods when type III and type II bursts were observed (Lincoln *et al.*, 1972). From Figure 9 the low energy X-ray burst (curves 1, 2 and 3) can be seen to begin shortly before the burst appearing at higher energies (curves 6, 7 and 8); the highest energy component reaches a maximum towards 1521 UT, and then drops very rapidly. The X-ray time profile, particularly at high energies, coincides fairly well with the shape of the microwave radio burst. Figure 10 shows the time correlation between our data, radio flux measurements and TD1 and Intercosmos 7 experiments where the time resolution was better (Van Beek *et al.*, 1973, Valnicek *et al.*, 1973). The two types of radiation typically show a 'step' profile in time with intermediary maxima 1516, 1517 30, 1519 UT (Figures 9 and 10). This is probably related to the intermediary maxima indicated above in the X-ray and radio ranges.

The radio observation data in the frequency range 245 to 15 400 MHz (Castelli *et al.*, 1973) indicate that the beginning of the radio burst may be situated at 1422 and the observable increase in frequencies 930 to 2800 MHz begins at 1505 UT, simultaneously with an increase in Hα line intensity (Lincoln *et al.*, 1972).

Beginning at 1519 UT a white light burst appears lasting 7 to 8 minutes from the moment of maximum intensity in the radio spectrum (Castelli *et al.*, 1973). A type II radio burst also appears which seems to begin at about 1521 UT and which lasts
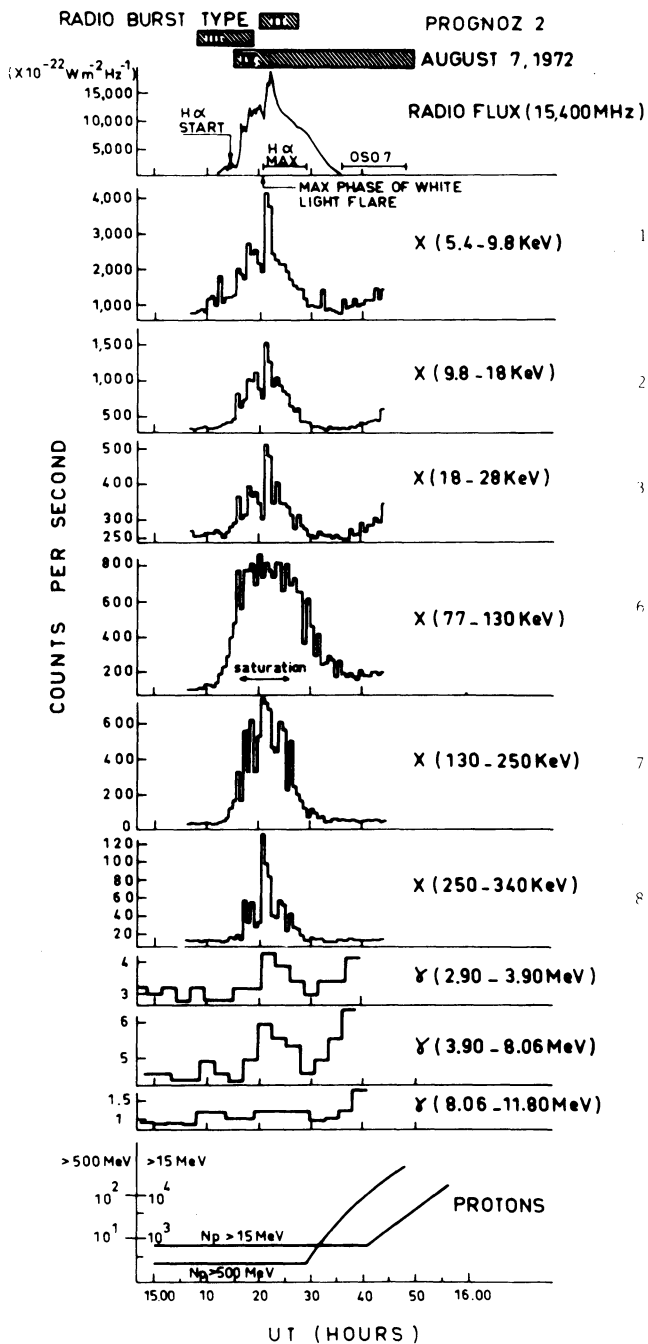
Fig. 9.   Time profiles of the X-ray, γ-ray and proton measurements in the August 7 event.

till 1535 UT (Dodge, 1973). At 1521 30 a flux maximum in the hard X-ray photon flux is noted almost simultaneous with an increase in the count rate in the range 2.9–7.8 MeV. The gamma burst lasts about 8 to 10 min.
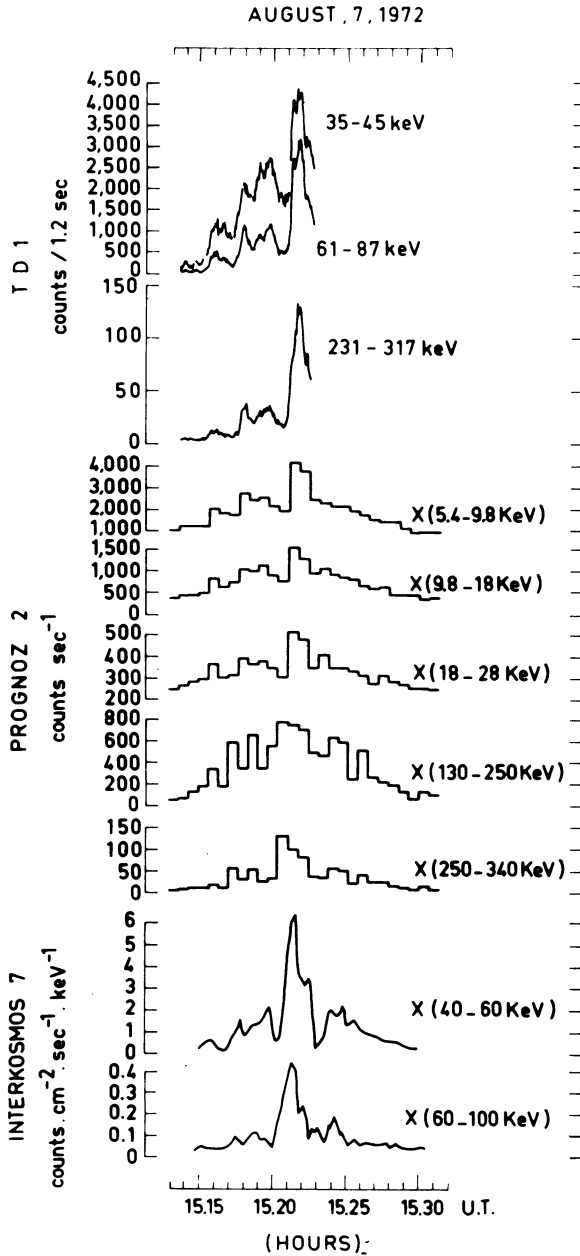

Fig. 10.   A detailed time profile of X-ray measurements in the August 7 event.

Since the X-ray measurements have a time resolution of 41 s it is not possible to show an accurate time correlation in the development of the photon fluxes for these two energy ranges. Nonetheless, the X- and gamma-events end at about 1527 UT, shortly before the high-energy protons appear.

The increase in intensity of these protons ($E_p \geqslant 500$ MeV) begins at 1529–1530, while the low energy charged particles (1 MeV $< E_p < 200$ MeV) appear only at about 1535 UT. Under these conditions the excess of the gamma ray fluxes between 1522 and 1530 cannot be interpreted as local production due to the arrival of protons. In addition we note that the arrival of protons coincides well with a very clear γ-ray flux increase which can be explained by local γ-ray production.

Chupp *et al.* (1973b) have already shown evidence for the 511 keV, 2.23 MeV, 4.43 MeV, and 6.1 MeV gamma lines related to positron annihilation, formation of deuterium, and excited states of C^{12} and O^{16} nuclei in these events. In our observations of this event, the spectral characteristics of the gamma-radiation were difficult to obtain due to the limited number of channels and to the measurement method. Nevertheless we shall try to analyze these data taking into account the contribution of the excited states of oxygen and carbon nuclei.

But first we shall comment on the time correlation in the different wavelength ranges. One of the most interesting results of the observational data is the correlation between type II radio bursts, and the arrival and time behavior of the energetic protons recorded over the gamma radiation which they produce in the flare region.

The radio bursts of this type usually appearing after large events result from the formation of a shock wave. For example in the August 4 event the type II radio burst at frequencies of 4824 MHz was observed between 0629 and 063305 (Castelli *et al.*, 1973), i.e. during the period of the gamma-burst. We can suppose at much higher frequencies this burst began a little earlier. However, a complex image of radio disturbances for this whole period makes it difficult to know the exact moment of the beginning of the type II burst.

In the August 7 event, the image of the correlation is clearer; the type II radio burst began at 1519 (according to data from different stations this moment can be determined to within $+1$ min, -0.3 min) (Lincoln *et al.*, 1972) and lasts until 1537. The gamma burst under observation began at 1522 and continued until 1530. The beginning of the burst is determined to within ± 1 min. Thus we can consider that between the start of the type II radio burst at 1519 and of the gamma burst at 1522, there was a certain time delay $t \simeq 10^2$ s which may indicate that the maximum proton flux density does not appear immediately after the shock wave formation.

Concerning time correlations between the event recorded in X- and γ-rays, we can note that the X- and γ-ray flux increases are simultaneous to within our time measurements errors. But when the X event lasts only about 2 min the γ-ray event extends over on period of about 8 to 10 min. This lack of correlation in the length of the 2 events is further evidence of a different origin for the X-rays (electron bremsstrahlung) and γ-ray fluxes (solar atmosphere proton interactions).

(ii) *Evaluation of a Possible Continuum Contribution above* 3 MeV

As we have just remarked time correlations between X- and γ-ray events seem to indicate a different origin for these emissions.

In spite of this argument, we have attempted to calculate the contribution of a continuum in channels ΔE_{14}, ΔE_{15}, ΔE_{16} taking into account the low energy measurements (< 340 keV) given by SGL 1 detector. So this estimate is very approximate because we have no spectral information between 340 keV and 3 MeV.
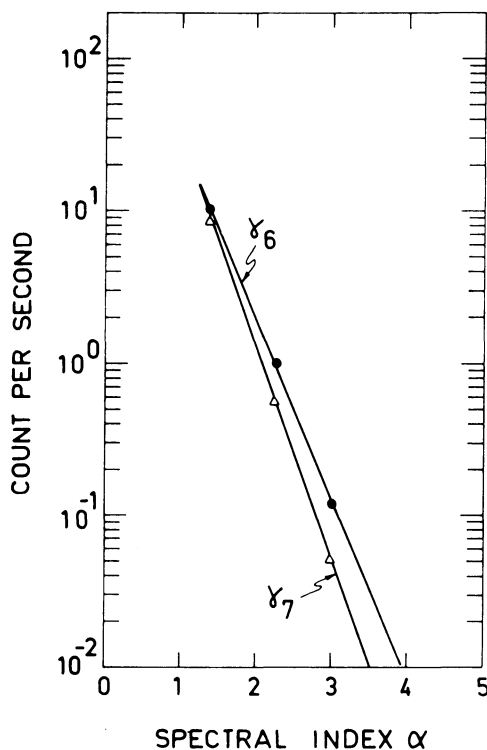

Fig. 11.   Counting rate in ΔE_{14} and ΔE_{15} vs. photon spectrum index α (normalized to channel 250–340 keV).

We have used the Monte Carlo program to calculate the contribution of the continuum in ΔE_{14}, ΔE_{15} for different slopes of this spectrum, the γ-ray spectrum being normalized to the value of the flux observed between 250 and 340 keV (Figure 11). If we retain a spectrum in E^{-3} which is rather close to that of the continuum for the August 4 event (Chupp *et al.*, 1974 – private communication), we notice that the expected gamma contribution is negligible compared with the counts observed. It must also be pointed out that whenever the exponent of the spectrum is greater than 1, it leads to contributions in ΔE_{14} and ΔE_{15} which are in ratio always greater than 1; for example, for $\alpha = 2.3$, $\Delta E_{14}/\Delta E_{15} = 2$, and this ratio increases at higher energy while $\Delta E_{14}/\Delta E_{15}$ observed during the event is 0.6 (Figure 11).

Let us further note that it is difficult to assume a spectrum of photons having a slope of less than 2 above 500 keV because the resulting gamma photon flux above 500 keV, would cause an increase in the anticoincidence count rate, which would be significant. However, no such systematic increase during the event was observed.

None of these arguments constitutes a definitive proof as to the absence of significant continuum contribution. It nevertheless seems clear that if we take a spectrum above 400 keV with a slope less than 2.5, the total count rate observed cannot be due to the continuum, the best proof still being the ratio of the fluxes observed in ΔE_{15} and ΔE_{16}.

Under these conditions, the presence of a contribution of monoenergetic gamma photons is reasonably possible. However, we can only give it as upper limit by supposing that the entire observed contribution is due to the presence of these lines. If a continuum exists, it can provide a contribution that is impossible to determine precisely, given the observational data at the time of the event.

(iii) *Evaluation of a Possible γ-Ray Line Contribution*

Calculations have been made under the assumption that only the 6.14 and 4.43 MeV lines are excited (Ramaty and Lingenfelter 1973). In fact perhaps the actual situation at the Sun is much more complicated than it is supposed here.

Due to poor time resolution the length of the event cannot be given exactly but lies between 8 and 11 min. Taking into account the detection efficiency for these two lines and using the Monte-Carlo program we have calculated the fluxes of 4.43 and 6.14 MeV γ-ray lines to be 1.8 and 0.7 photon $cm^{-2}\ s^{-1}$ respectively for a γ-ray burst lasting 8 min.

We can try to check if these γ-ray line fluxes are in agreement with those measured by Chupp *et al.* (1973a) on OSO 7. But as these measurements are obtained later we have to consider the time evolution of the 2.23 MeV flux to estimate what the 2.23 MeV flux would have been at the moment of our measurements. For simplification we can choose a time evolution for the 2.23 MeV flux given by $\exp[-\lambda(t-t_0)]$ with $\lambda = \tau_c^{-1} + \tau_d^{-1}$ where τ_c is the capture time of neutrons on hydrogen and τ_d the mean neutron lifetime (Reppin *et al.*, 1973). In this case we neglect the dependence of ϕ on θ and E_n (Wang en Ramaty, 1974), (θ is the angle between the Earth-Sun line and the vertical to the plane stratified medium; E_n is the neutron energy). The capture time τ_c is ~ 100 s. for a density of the ambient solar atmosphere $n = 10^{17}\ cm^{-3}$ if we use the expression $\tau_c(s) \simeq (1.5 \times 10^{19}/n(cm^{-3}))$ (Wang and Ramaty, 1974).

The 2.2 MeV γ-ray line at the end of the neutron production is given by ϕ_{t0}:

$$\phi_{t0} = \phi_t \exp\left[-\lambda(t-t_0)\right]. \tag{12}$$

Since the radio and X-ray measurements seem to indicate that the event ends at 1530 we may suppose that the neutron production also ends at this time. So if we take for ϕ_t the 2.23 MeV γ-ray flux measured by OSO 7 at about 1538 ($\phi_t \simeq 4.8 \times 10^{-2}$ $cm^{-2}\ s^{-1}$) we obtain for $\phi_{t0} \sim 2$ photons $cm^{-2}\ s^{-1}$.

With these values of ϕ and a rigidity of ~ 50 MV for the event, the calculations of Ramaty *et al.* (1973) give a ratio of ~ 3 between the γ-ray lines at 2.2 and 4.4 MeV for the thick target model. If we take into account the revised γ-ray fluxes at 2.23 MeV (Wang and Ramaty, 1974), which are lower than the values already published by a factor 2–2.5, the ratio $\phi_{2.2}/\phi_{4.4} \simeq 1.2$ to 1.5 for 50 MV rigidity. In this case we have a reasonably good agreement between theoretical calculations and our measurements at the end of the event at about 1530.

We shall now compare Ramaty's theoretical estimates with our experimental results in order to evaluate some of the basic parameters of the solar flare. But before that we need to determine the rigidity of the protons spectrum.

(α) *Determination of the event's characteristic rigidity.* This rigidity is defined as for the August 2 event using the measurements made by Bostrom *et al.* (1972). For the August 7 event we have the following values:

$$J (> 10 \text{ MeV}) = 4.2 \times 10^4 \, p \, \text{cm}^{-2} \, \text{s}^{-1}$$
$$J (> 30 \text{ MeV}) = 4.56 \times 10^3 \, p \, \text{cm}^{-2} \, \text{s}^{-1} \qquad (13)$$
$$J (> 60 \text{ MeV}) = 8.4 \times 10^2 \, p \, \text{cm}^{-2} \, \text{s}^{-1}$$

From Equation (7) the characteristic proton rigidity can be seen to be between 40 and 50 MV, which corresponds to densities of $U(> 10 \text{ MeV}) = 7.24 \times 10^{-6} \text{ cm}^{-3}$, $U(> 30 \text{ MeV}) = 5 \times 10^{-7} \text{ cm}^{-3}$, and $U(> 60 \text{ MeV}) = 6.8 \times 10^{-8} \text{ cm}^{-3}$, for an average characteristic rigidity of 45 MV. When curves $f(P)$ (Figure 12) are plotted, the values 40 and 50 MV corresponding to the slopes of these curves do reflect the average value of 45 MV. The particle rigidity derived from these observations is thus included between 40 and 50 MV. The results based on this and using of Ramaty's and Lingenfelter's calculations appear below.

We have to note, however, that the following estimates depend strongly on the characteristics of the proton spectra. In particular, the high values of the number of protons in the thick-target model, the density of the region where the γ-photons are produced in the thin-target model, and the energies involved would be reduced by an order of magnitude if the rigidity reached 100 MV.

(β) *Number of protons involved in the flare.* According to Figure 7 we obtain the following photons fluxes normalized to one proton:

Proton rigidity	4.43 MeV	6.14 MeV
40 MV	3.3×10^{-34}	2.4×10^{-34}
50 MV	8.7×10^{-34}	5.7×10^{-34}

$$(14)$$

Since the total fluxes at 4.43 MeV and 6.14 MeV are respectively 883 photons cm^{-2}
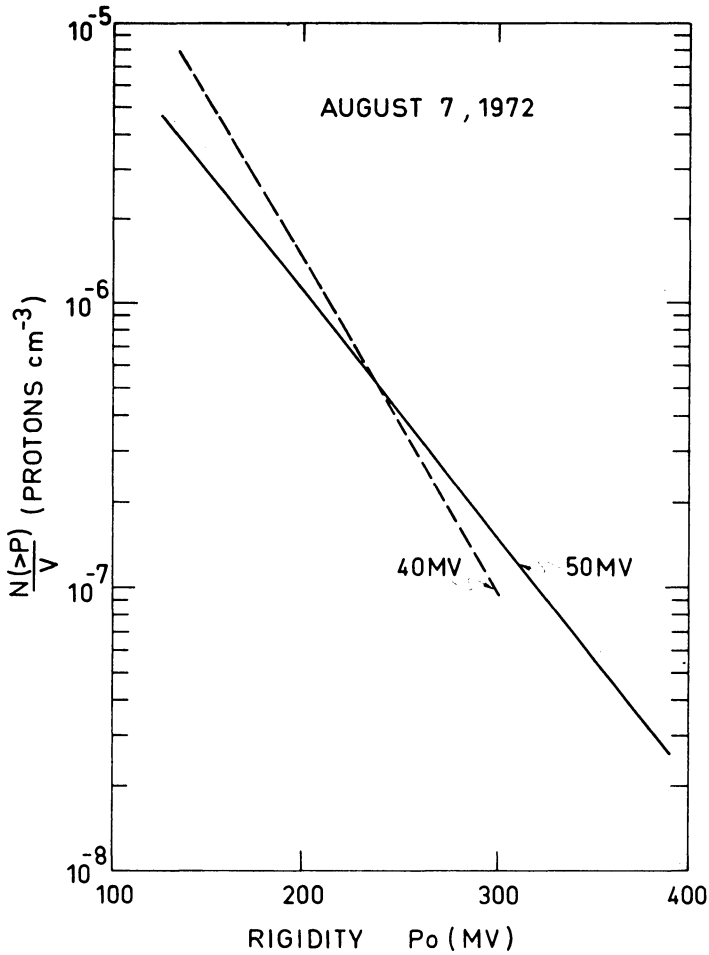
Fig. 12. Density of protons near the Earth vs rigidity for 2 characteristic rigidities in the 1972, August 7 event.

and 331 photons cm^{-2}, from Ramaty's curve it is possible to estimate the number of protons involved in the event:

Proton rigidity	4.43 MeV	6.14 MeV	Average value	
40 MV	2.7×10^{36}	1.4×10^{36}	2.0×10^{36}	(15)
50 MV	1.0×10^{36}	5.8×10^{35}	8.0×10^{35}	

From Figure 12 one can obtain the proton density in interplanetary space, and the proton flux at the Sun can be deduced:

$$2.5 \times 10^{35} < N(P > 0) < 5.6 \times 10^{34} \quad \text{for} \quad 40\,\text{MV} < P_0 < 50\,\text{MV} \quad (16)$$

This estimate is made on the assumption that the volume occupied by the particles in interplanetary space is a cone with a 30° opening angle whose vertex is on the Sun (Ramaty and Lingenfelter, 1973). This volume is estimated to be 10^{39} cm^3. These two determinations of the proton flux at the Sun are not in good agreement.

(γ) *Density in the solar atmosphere deduced from the thin target model.* From Figure 6 we find the number of photons produced by one proton in a solar atmosphere having a density of 1 cm^{-3}.

Proton rigidity	4.43 MeV	6.14 MeV	
40 MV	9.4×10^{-48}	6.9×10^{-48}	(17)
50 MV	1.7×10^{-47}	1.2×10^{-47}	

Since the photon fluxes measured are 1.8 photons cm^{-2} s^{-1} at 4.43 MeV and 0.7 photons cm^{-2} s^{-1} at 6.14, we can estimate the product nN expressed in cm^{-3}, i.e.

Proton rigidity	4.43 MeV	6.14 MeV	
40 MV	1.9×10^{47}	1.0×10^{47}	(18)
50 MV	1.1×10^{47}	5.8×10^{46}	

The number of protons N is obtained by estimates given above: $N = 2.5 \times 10^{35}$ for $P_0 = 40$ MV and 5.6×10^{34} for $P_0 = 50$ MV. The density encountered by the protons at the Sun for the creation of measured photon fluxes is given in the following table:

Proton rigidity	4.43 MeV	6.14 MeV	Average value	
40 MV	7.9×10^{11}	4.0×10^{11}	6.0×10^{11}	(19)
50 MV	1.9×10^{12}	1.0×10^{12}	1.5×10^{12}	

(δ) *Energy involved in the flare.* First we consider the thick-target case. For a spectrum having the form $P_0^{-1} \exp(-P/P_0)$ and for non relativistic protons, the average proton energy is P_0^2/Mc^2; thus for the thick-target model the energies carried by 2×10^{36} protons and 8×10^{35} protons are 5.6×10^{30} erg and 3.5×10^{30} ergs for 40 and 50 MV respectively.

For the thin target model the rate of gamma photon production and the proton energy loss rate depend on the product of the ambient density and the number of protons emitted (Ramaty and Lingenfelter, 1973). The ratio of these two rates is independent of n and N depends on the accelerated proton spectrum, i.e. on P_0. Table V gives the energy lost by a proton with rigidity above 0 for $n = 1$ cm^{-3} and for various characteristic rigidities.

Between 40 and 50 MV, W is about 1.9×10^{-18} erg s^{-1} (Table V). Using the values for n and N given above, for the energy involved expressed in erg s^{-1} we have:

Proton rigidity	4.43 MeV	6.14 MeV	Average value	
40 MV	3.7×10^{29}	1.9×10^{29}	2.8×10^{29}	(20)
50 MV	2.1×10^{29}	1.1×10^{29}	1.6×10^{29}	

Since the event lasted 8 min, the total energy involved, expressed in ergs, is:

Proton rigidity	4.43 MeV	6.14 MeV	Average value	
40 MV	1.8×10^{32}	9.1×10^{31}	1.3×10^{32}	(21)
50 MV	1.0×10^{32}	5.5×10^{31}	7.7×10^{31}	

This corresponds to an average energy 1.2×10^{32} ergs involved in the entire γ-ray event.

III. Conclusion

After a general description of the 2 events on August 2 and 7, we have tried to present some evidence of the presence of γ-ray lines during these two events. It seems that for the August 2 event a line at 0.511 MeV is revealed but this does not exclude definitively the possibility of an X-ray continuum extending to about 600 keV. For the August 7 event, the evidence of high energy γ-rays up to 8 MeV is clearly shown, but as we have no spectral information between 500 keV and 3 MeV it is still difficult to estimate a continuum γ-ray contribution. We have nevertheless attempted to do it, but our results seem to be more consistent with the presence of lines at 4.43 and 6.14 MeV, if the Ramaty-Lingenfelter theory is used. Obviously without the support of this theory, it will be impossible to say anything about the origin of the observed γ-ray excess.

In any case it appears that the durations for the X- and γ-ray emission during the 7 August event are quite different, which seems to indicate a different origin for these emissions. In fact this is quite possible, even if there is only continuum, because, as Chupp et al. (1972) point out the origin of this continuum may not be entirely related to the presence of high energy electron bremsstrahlung and other lines, not resolved and associated with proton interactions, may contribute.

If as we think the excess of γ-ray flux recorded by our experiment can be attributed to proton interactions in solar atmosphere, the reasonably good time correlation at the beginning of the X- and γ-ray events seems to prove that the non-relativistic and mildly relativistic energy electrons are accelerated at about the same time as the relativistic electron and high energy protons (Švestka, 1973).

Acknowledgements

References

Blioudov, V. A., Voloditchev, N. N., Grigorov, N. L., Kusine, Y. N., Likine, O. B., Netchaev, Y. Y., Podolsky, A. N., Savenko, I. A., Suslov, A. A., Ustinov, V. M., and Dritchikov, X.: 1974, *Geomagnetism i Aeronomiya* **13**, 1029.

Bostrom, C. O., Kohl, J. W., Mc Entire, R. W., and Williams, D. J.: 1972, 'The Solar Protons Flux – August 2–12, 1972', Preprint, The Johns Hopkins University, Silver Spring, Maryland.

Brown, T.: 1972, *Solar Phys.* **26**, 441.

Bui-Van, A., Giordano, G., Hurley, K., and Mandrou, P.: 1973, 'A Monte Carlo Program for Scintillation Counter Response, C.E.S.R. report 73–382 – August.

Castelli, T. P., Barron, W. R., and Aarons, T.: 1973, Solar Radio Activity in August 1972, AFCRL-TR-73-0086.

Chupp, E. L., Forrest, D. J., and Suri, A. N.: 1972, 'Solar Gamma Ray and Neutron Observations', Max Planck Institut für Physik and Astrophysik – M.P.I.-PAE/Extraterr. 77.

Chupp, E. L., Forrest, D. J., and Suri, A. N.: 1973a, Gamma Ray and Neutron Measurements and Their Relation to the Solar Flare Problem', 16th Meeting of Cospar, Konstanz, May–June.

Chupp, E. L., Forrest, D. J., Higbie, P. R., Suri, A. N., Tsai, C., and Dunphy, P. P.: 1973b, *Nature* **241**, 333.

Chupp, E. L., Forrest, D. J., and Suri, A. N.: 1974, Private communication.

Datlowe, D. W. and Peterson, L. E.: 1973, 'OSO-7 Observation of Solar X-Ray Bursts from 28 July to 9 August 1972', Report UAG-28, II, 291.

Dodge, J. C.: 1973, 'Interferometric Radio Spectrum of the Solar Corona, 1–11 August 1972 in Collected Data Reports on August 1972 – Solar Terrestrial Events', World Data Center, A, Report UAG-28, Part I, 242.

Grigorov, N. L., Melioransky, A. S., Nazarov, N. N., Pankov, V. M., Savenko, I. A., and Spirnov, S. P.: 1974, *Geomagnetism i Aeronomiya*, (in press).

Kudriavtsev, M. I., Likine, O. B., Melioransky, A. S., Savenko, I. A., Smirnov, V. V., and Chamoline, V. M.: 1973, *Geomagnetism i Aeronomiya* **13**, 406.

Lincoln, J. V. and Leighton, H. J.: 1972, 'Preliminary Compilation of Data for Retrospective World Interval July 26–August 14, 1972', World Data Center A., Report UAG-21, 1972a.

Ramaty, R. and Lingenfelter, R. E.: 1973, Nuclear Gamma Rays from Solar Flare, NASA X-660-73-14.

Reppin, C., Chupp, E. L., Forrest, D. J., and Suri, A. N.: 1973, 'Solar Neutron Production during the Events on 04 and 07 August 1972', *13th Int. Cosmic Ray Conf.*, Denver, August 1973.

Straka, R. M.: 1970, 'The Use of Solar Radio Bursts as Predictors of Proton Event Magnitude, AFCRL Space Forecasting Research Note, June 1970.

Švestka, Z.: 1973, 'Critical Problems of Solar Flare Research', 16th Meeting of Cospar, Konstanz, May–June.

Valnicek, B., Farnik, F., Horn, J., Letfus, V., Sudova, J., Komarek, B., Engelthaler, P., Ulrych, J., Moucka, L., Fronka, O., Vasek, T., Beranek, I., Pich, J., and Zderadicka, J.: 1973, *Bull. Astro. Inst. Czech.* **24**, No. 6.

Van Beek, H. F., Hoyng, P., and Stevens, G. A.: 1973, 'Solar Flares Observed by the Hard X-Ray Spectrometer on Board the ESRO TD1-A Satellite', Report UAG-28, II, 319.

Vedrenne, G., Talon, R., and Cotin, F.: 1973, 'Experience SIGNE 1', – C.E.S.R. Report 73–364, Avril, Toulouse, France.

Wang, H. T. and Ramaty, R.: 1974, *Solar Phys.* **36**, 129.

Zirin, H. and Tanaka, K.: 1973, *Solar Phys.* **32**, 173.